



Article

Hermite Fitted Block Integrator for Solving Second-Order Anisotropic Elliptic Type PDEs

Emmanuel Oluseye Adeyefa ¹, Ezekiel Olaoluwa Omole ¹, Ali Shokri ² and Shao-Wen Yao ^{3,*}

¹ Department of Mathematics, Faculty of Science, Federal University Oye-Ekiti, P.M.B. 373, Oye-Ekiti 370112, Ekiti State, Nigeria; adeoluman@yahoo.com (E.O.A.); omolez247@gmail.com (E.O.O.)

² Faculty of Mathematical Sciences, University of Maragheh, Maragheh 83111-55181, Iran; shokri@maragheh.ac.ir

³ School of Mathematics and Information Science, Henan Polytechnic University, Jiaozuo 454000, China

* Correspondence: yaoshaowen@hpu.edu.cn

Abstract: A Hermite fitted block integrator (HFBI) for numerically solving second-order anisotropic elliptic partial differential equations (PDEs) was developed, analyzed, and implemented in this study. The method was derived through collocation and interpolation techniques using the Hermite polynomial as the basis function. The Hermite polynomial was interpolated at the first two successive points, while the collocation occurred at all the suitably chosen points. The major scheme and its complementary scheme were united together to form the HFBI. The analysis of the HFBI showed that it had a convergence order of eight with small error constants, was zero-stable, absolutely-stable, and satisfied the condition for convergence. In order to confirm the usefulness, accuracy, and efficiency of the HFBI, the method of lines approach was applied to discretize the second-order anisotropic elliptic partial differential equation PDE into a system of second-order ODEs and consequently used the derived HFBI to obtain the approximate solutions for the PDEs. The computed solution generated by using the HFBI was compared to the exact solutions of the problems and other existing methods in the literature. The proposed method compared favorably with other existing methods, which were validated through test problems whose solutions are presented in tabular form, and the comparisons are illustrated in the curves.

Keywords: anisotropic elliptic PDEs; block integrator; collocation strategy; convergence analysis; discretization; hermite fitted; second-order PDEs; system of second-order ODEs

MSC: 65M12; 65M20



Citation: Adeyefa, E.O.; Omole, E.O.; Shokri, A.; Yao, S.-W. Hermite Fitted Block Integrator for Solving Second-Order Anisotropic Elliptic Type PDEs. *Fractal Fract.* **2022**, *6*, 497. <https://doi.org/10.3390/fractalfract6090497>

Academic Editors: Sotiris K. Ntouyas, Jessada Tariboon and Bashir Ahmad

Received: 19 July 2022

Accepted: 29 August 2022

Published: 5 September 2022

Publisher's Note: MDPI stays neutral with regard to jurisdictional claims in published maps and institutional affiliations.



Copyright: © 2022 by the authors. Licensee MDPI, Basel, Switzerland. This article is an open access article distributed under the terms and conditions of the Creative Commons Attribution (CC BY) license (<https://creativecommons.org/licenses/by/4.0/>).

1. Introduction

An anisotropic equation is an example of a second-order elliptic partial differential equation with broad applications in theoretical physics, applied mathematics, engineering, and other fields of study [1]. In [2], the regularization Cauchy problem for matrix factorizations of the Helmholtz equation in a multidimensional bounded domain was discussed. Similarly, Ref. [3] examined the Cauchy problem for degenerate parabolic convolution equations. The asymptotic reduction in the solution space dimension and applications in dynamical systems were proposed in [4]. The solution of fractional differential equations is explored through Geraghty type hybrid contractions in [5], the solution of differential equations through the New integral operator was studied by [6,7] presented a variable compact multipoint upscaling scheme for anisotropic diffusion problems in three dimensions. In this paper, we consider a second-order anisotropic elliptic partial differential equation of the form

$$\nabla^2 u = g(x, y), \quad (1)$$

Over the years, the numerical solution of Equation (1) has become of great importance to scholars and scientists due to its practical applications in applied mathematics and

engineering. The second-order elliptic partial differential equations of the form (1) are usually modeled into linear or nonlinear equations [8]. These types of problems are widely used to model real-life problems, for instance, the transportation of oxygen in a tissue plate at a constant rate of oxygen consumption [9], certain non-smooth oscillators with large nonlinearities with periodic solutions [10], elastohydrodynamic lubrication [11], electromagnetic scattering theory, the flow of air pollutants, velocity potential, micro- and nano-electronic devices in physics [12], the boussinesq-love equation's inverse boundary value problem with the nonlocal integral condition [13], the modeling of coupled dynamic thermoelastic issues for isotropic solids using mathematics and computers [14], and the estimation of the stability for the difference and delay parabolic equations [15]. As a result, most of these problems or models do not have an exact solution. This results in the fact that it is usually difficult to solve some of these equations or problems analytically. Thus, there is the need to employ an appropriate numerical method to solve them numerically.

Many numerical models have been proposed for the numerical approximation of Equation (1), while some have been developed for the theoretical solutions of (1). Many real-life situations or experimental equations cannot be solved analytically. Therefore, numerical techniques are employed for the numerical approximation of such problems. A countless number of numerical algorithms have been constructed for solving (1). Such techniques include the Adomian Decomposition methods [16,17], the Haar wavelet method [18], trigonometrically fitted block techniques [19,20], the variational homotopy perturbation method [21], the direct solver approach [22], block algorithms [23–27], the finite difference method [28]; transform techniques [29], the Legendre-homotopy method [30], and the cubic spline method [31,32].

The search for numerical methods with better accuracy led us to this present work. In this article, the Hermite fitted block integrator HFBI for solving a class of (1) which is assumed to satisfy the existence and uniqueness of solution within the interval of domain of integration, is proposed. The HFBI possessed a convergent order of eight. We are motivated to propose HFBI as a result of the outstanding features of the block integrator, including that it is more efficient, has good stability properties, and possesses high convergence. This enormous success of block integrators has greatly removed the burden of developing predictors separately, the complexity in computing, the slow convergence, instability, and computational time.

The remaining part of the article is designed as follows: Section 1 defines the introduction, area of applications, and the related literature review. Section 2 details the mathematical formulation of the HFBI. The properties of the HFBI such as order and error, consistency, zero-stability, and the region of absolute stability are analyzed in Section 3. Furthermore, the computational strategy is outlined in Section 4. The numerical examples, comparison of the numerical results of HFBI with the results of existing methods are presented, along with the comparison in curves in Section 5. Finally, the conclusions are discussed based on the numerical results to verify the accuracy, reliability, and efficiency of HFBI in Section 6.

2. Methodology

In this section, we discuss in details the mathematical formulation of HFBI for the numerical solution of (1) where

$$\nabla^2 u = \epsilon \frac{\partial^2 u}{\partial x^2}(x, y) + \frac{\partial^2 u}{\partial y^2}(x, y),$$

for all $(x, y) \in \Omega \subseteq \mathbb{R}^2$, where $\Omega = \{(x, y) : (x, y) \in [a, b] \times [c, d]\}$ with boundary $\partial\Omega$. Related to (1) are the initial conditions

$$u(x, a) = v_1(x), \quad \frac{\partial u}{\partial y}(x, b) = v_2(x), \quad x \in [a, b], \quad (2)$$

or the Dirichlet boundary conditions

$$u(x, c) = v_3(x), \quad u(x, d) = v_4(x), \quad x \in [c, d]. \quad (3)$$

With respect to (1), the solution $u(x, y)$ is termed the dependent variable, $g(x, y)$ is called the forcing function, and x and y are the spatial variables. $\epsilon < 1$ or $\epsilon > 1$ for all $(x, y) \in \Omega$. In addition, Ω is a rectangular domain with appropriate boundary and initial conditions. The variables functions are assumed to be a continuous functions that satisfy the necessary conditions for the existence and uniqueness. The theorems that provide the conditions are discussed extensively in [33,34].

Mathematical Formulation of the HFBI

Here, the numerical solution of (1) is sought on the interval x_n to x_{n+7} by a Hermite polynomial of the form

$$u(x) = \sum_{i=0}^{k+2} c_i H_i(x), \quad i = 0, 1 \quad (4)$$

where (H_i) are probabilists Hermite polynomials generated by the recursive relation and step-number ($k = 7$).

$$H_{n+1}(x) = xH_n(x) - H'_n(x)$$

The first six probabilists Hermite polynomials [35] are

$$\left. \begin{aligned} H_0(x) &= 1 \\ H_1(x) &= x \\ H_2(x) &= x^2 - 1 \\ H_3(x) &= x^3 - 3x \\ H_4(x) &= x^4 - 6x^2 + 3 \\ H_5(x) &= x^5 - 10x^3 + 15x \end{aligned} \right\}$$

$$u''(x) = \sum_{i=2}^{k+2} c_i H''_i(x), \quad i = 2, 3, \dots, k+2 \quad (5)$$

where $k+2 = c + r - 1$, r is the interpolation points, and c is the collocation point. Equation (4) is referred to as the interpolation equation, whereas (5) is the collocation equation. Imposing the following conditions on (4) and (5) gives

$$u_{m+j,n} = \sum_{i=0}^{k+2} c_i H_i(x), \quad i, = 0, 1 \quad (6)$$

$$f_{m+j,n} = \sum_{i=2}^{k+2} c_i H''_i(x), \quad i, = 2(1)k+2 \quad (7)$$

The Equations (6) and (7) are joined together to form a system of $c + r - 1$ equations, which is represented by

$$LC = W \quad (8)$$

where

$$L = \begin{bmatrix} H_0(x_n) & H_1(x_n) & H_2(x_n) & H_3(x_n) & \cdots & H_{k+2}(x_n) \\ H_0(x_{n+1}) & H_1(x_{n+1}) & H_2(x_{n+1}) & H_3(x_{n+1}) & \cdots & H_{k+2}(x_{n+1}) \\ H_0''(x_n) & H_1''(x_n) & H_2''(x_n) & H_3''(x_n) & \cdots & H_{k+2}''(x_n) \\ H_0''(x_{n+1}) & H_1''(x_{n+1}) & H_2''(x_{n+1}) & H_3''(x_{n+1}) & \cdots & H_{k+2}''(x_{n+1}) \\ \vdots & \vdots & \vdots & \vdots & \cdots & \vdots \\ \vdots & \vdots & \vdots & \vdots & \cdots & \vdots \\ H_0''(x_{n+k}) & H_1''(x_{n+k}) & H_2''(x_{n+k}) & H_3''(x_{n+k}) & \cdots & H_{k+2}''(x_{n+k}) \end{bmatrix}$$

$$C = \begin{bmatrix} c_0 \\ c_1 \\ c_2 \\ c_3 \\ \vdots \\ c_{k+2} \end{bmatrix} \quad W = \begin{bmatrix} u_{m,n} \\ u_{m+1,n} \\ f_{m,n} \\ f_{m+1,n} \\ \vdots \\ f_{m+k,n} \end{bmatrix}$$

Matrix Equation (8) is solved for the unknown values of $c_i, i = 0(1)9$ using Maple 18.0. The values (see Appendix A) are then placed into (4) to obtain the continuous implicit equation together with its derivative in the form

$$u_{m+j,n}(t) = \gamma_0(t)u_{m,n} + \gamma_1(t)u_{m+1,n} + h^2 \sum_{j=0}^{k+2} \psi_j(t)f_{m+j,n}, \quad j = 0(1)k+2 \quad (9)$$

where

$$u_{m,n} = u(x_n), \quad u_{m+1,n} = u(x_{n+1}), \quad f_{m+j,n} = f\left(x_{m+j,n}, u_{m+j,n}, u'_{m+j,n}\right),$$

$$t = \left(\frac{x - x_{n+6}}{h}\right)$$

$$\left\{ \begin{array}{l} \gamma_0(t) = (-t - 5) \\ \gamma_1(t) = (t + 6) \\ \psi_0(t) = -\frac{h^2 s}{1,814,400} (5t^7 + 35t^6 + 65t^5 - 85t^4 - 133t^3 - 607t^2 + 3467t - 19,927) \\ \psi_1(t) = \frac{h^2 s}{1,814,400} (35t^7 + 290t^6 + 500t^5 - 340t^4 - 3196t^3 + 7556t^2 - 47,716t + 298,196) \\ \psi_2(t) = -\frac{h^2 s}{604,800} (35t^7 + 335t^6 + 665t^5 - 565t^4 - 2521t^3 - 679t^2 + 7499t - 62,119) \\ \psi_3(t) = \frac{h^2 s}{362,880} (35t^7 + 380t^6 + 950t^5 - 766t^4 - 2938t^3 - 982t^2 - 1858t + 49,898) \\ \psi_4(t) = -\frac{h^2 s}{362,880} (35t^7 + 425t^6 + 1355t^5 - 439t^4 - 5455t^3 + 1355t^2 - 2455t - 13,645) \\ \psi_5(t) = -\frac{h^2 s}{604,800} (35t^7 + 470t^6 + 1880t^5 + 920t^4 - 8056t^3 - 7024t^2 + 16,544t + 28,736) \\ \psi_6(t) = -\frac{h^2 s}{1,814,400} (35t^7 + 515t^6 + 2525t^5 + 3815t^4 - 5701t^3 - 22,339t^2 - 21,721t + 1901) \\ \psi_7(t) = \frac{h^2 s}{1,814,400} (5t^7 + 80t^6 + 470t^5 + 1250t^4 + 1382t^3 + 218t^2 - 658t + 698) \\ s = (t + 6)(t + 5) \end{array} \right. \quad (10)$$

$$AU_M = B_MR_0 + B_{MM}R_1 + h^2[D_MR_2 + E_MR_3] \quad (11)$$

$$A = \begin{bmatrix} -120,960 & 60,480 & 0 & 0 & 0 & 0 & 0 \\ -181,440 & 0 & 60,480 & 0 & 0 & 0 & 0 \\ -120,960 & 0 & 0 & 30,240 & 0 & 0 & 0 \\ -151,200 & 0 & 0 & 0 & 30,240 & 0 & 0 \\ -362,880 & 0 & 0 & 0 & 0 & 60,480 & 0 \\ -60,480 & 0 & 0 & 0 & 0 & 0 & 8640 \\ -1,814,400 & 0 & 0 & 0 & 0 & 0 & 0 \end{bmatrix}, U_M = \begin{bmatrix} u_{m+1,n} \\ u_{m+2,n} \\ u_{m+3,n} \\ u_{m+4,n} \\ u_{m+5,n} \\ u_{m+6,n} \\ u_{m+7,n} \end{bmatrix}$$

$$B_M = \begin{bmatrix} 0 & 0 & 0 & 0 & 0 & 0 & 60,480 \\ 0 & 0 & 0 & 0 & 0 & 0 & 120,960 \\ 0 & 0 & 0 & 0 & 0 & 0 & 90,720 \\ 0 & 0 & 0 & 0 & 0 & 0 & 120,960 \\ 0 & 0 & 0 & 0 & 0 & 0 & 302,400 \\ 0 & 0 & 0 & 0 & 0 & 0 & 51,840 \\ 0 & 0 & 0 & 0 & 0 & 0 & 1,814,400 \end{bmatrix}, R_0 = \begin{bmatrix} u_{m-1,n} \\ u_{m-2,n} \\ u_{m-3,n} \\ u_{m-4,n} \\ u_{m-5,n} \\ u_{m-6,n} \\ u_{m,n} \end{bmatrix}$$

$$B_{MM} = \begin{bmatrix} 0 & 0 & 0 & 0 & 0 & 0 & 0 \\ 0 & 0 & 0 & 0 & 0 & 0 & 0 \\ 0 & 0 & 0 & 0 & 0 & 0 & 0 \\ 0 & 0 & 0 & 0 & 0 & 0 & 0 \\ 0 & 0 & 0 & 0 & 0 & 0 & 0 \\ 0 & 0 & 0 & 0 & 0 & 0 & 0 \\ 0 & 0 & 0 & 0 & 0 & 0 & 1,814,400 \end{bmatrix}, R_1 = \begin{bmatrix} u'_{m-1,n} \\ u'_{m-2,n} \\ u'_{m-3,n} \\ u'_{m-4,n} \\ u'_{m-5,n} \\ u'_{m-6,n} \\ u'_{m,n} \end{bmatrix}$$

$$D_M = \begin{bmatrix} 0 & 0 & 0 & 0 & 0 & 0 & 4125 \\ 0 & 0 & 0 & 0 & 0 & 0 & 8060 \\ 0 & 0 & 0 & 0 & 0 & 0 & 6013 \\ 0 & 0 & 0 & 0 & 0 & 0 & 7996 \\ 0 & 0 & 0 & 0 & 0 & 0 & 19,927 \\ 0 & 0 & 0 & 0 & 0 & 0 & 3436 \\ 0 & 0 & 0 & 0 & 0 & 0 & -416,173 \end{bmatrix}, R_2 = \begin{bmatrix} f_{m-1,n} \\ f_{m-2,n} \\ f_{m-3,n} \\ f_{m-4,n} \\ f_{m-5,n} \\ f_{m-6,n} \\ f_{m,n} \end{bmatrix}$$

$$E_M = \begin{bmatrix} 55,324 & -6297 & 14,598 & -11,477 & 5568 & -1551 & 190 \\ 116,293 & 37,410 & 33,539 & -21,656 & 10,299 & -2854 & 349 \\ 88,412 & 43,815 & 50,374 & -12,661 & 7296 & -2063 & 254 \\ 118,693 & 68,706 & 87,235 & 9640 & 12,699 & -2918 & 349 \\ 298,196 & 186,357 & 249,490 & 68,225 & 86,208 & -1901 & 698 \\ 51,065 & 34,410 & 44,719 & 18,824 & 20,103 & 8194 & 689 \\ -950,684 & 1,025,097 & -1,059,430 & 768,805 & -362,112 & 99,359 & -12,062 \end{bmatrix}, R_3 = \begin{bmatrix} f_{m+1,n} \\ f_{m+2,n} \\ f_{m+3,n} \\ f_{m+4,n} \\ f_{m+5,n} \\ f_{m+6,n} \\ f_{m+7,n} \end{bmatrix}$$

We proceed by multiplying Equation (11) by the reciprocal of matrix A, which gives the following HFBI of the form

$$A^{-1}AU_M = A^{-1}B_MR_0 + A^{-1}B_{MM}R_1 + h^2[A^{-1}D_MR_2 + A^{-1}E_MR_3] \quad (12)$$

$$A^{-1}A = I = \begin{bmatrix} 1 & 0 & 0 & 0 & 0 & 0 & 0 \\ 0 & 1 & 0 & 0 & 0 & 0 & 0 \\ 0 & 0 & 1 & 0 & 0 & 0 & 0 \\ 0 & 0 & 0 & 1 & 0 & 0 & 0 \\ 0 & 0 & 0 & 0 & 1 & 0 & 0 \\ 0 & 0 & 0 & 0 & 0 & 1 & 0 \\ 0 & 0 & 0 & 0 & 0 & 0 & 1 \end{bmatrix}, U_M = \begin{bmatrix} u_{m+1,n} \\ u_{m+2,n} \\ u_{m+3,n} \\ u_{m+4,n} \\ u_{m+5,n} \\ u_{m+6,n} \\ u_{m+7,n} \end{bmatrix}$$

$$A^{-1}B_M = \begin{bmatrix} 0 & 0 & 0 & 0 & 0 & 0 & 1 \\ 0 & 0 & 0 & 0 & 0 & 0 & 1 \\ 0 & 0 & 0 & 0 & 0 & 0 & 1 \\ 0 & 0 & 0 & 0 & 0 & 0 & 1 \\ 0 & 0 & 0 & 0 & 0 & 0 & 1 \\ 0 & 0 & 0 & 0 & 0 & 0 & 1 \\ 0 & 0 & 0 & 0 & 0 & 0 & 1 \end{bmatrix}, R_0 = \begin{bmatrix} u_{m-1,n} \\ u_{m-2,n} \\ u_{m-3,n} \\ u_{m-4,n} \\ u_{m-5,n} \\ u_{m-6,n} \\ u_{m,n} \end{bmatrix}$$

$$A^{-1}B_{MM} = \begin{bmatrix} 0 & 0 & 0 & 0 & 0 & 0 & 1 \\ 0 & 0 & 0 & 0 & 0 & 0 & 2 \\ 0 & 0 & 0 & 0 & 0 & 0 & 3 \\ 0 & 0 & 0 & 0 & 0 & 0 & 4 \\ 0 & 0 & 0 & 0 & 0 & 0 & 5 \\ 0 & 0 & 0 & 0 & 0 & 0 & 6 \\ 0 & 0 & 0 & 0 & 0 & 0 & 7 \end{bmatrix}, R_1 = \begin{bmatrix} u'_{m-1,n} \\ u'_{m-2,n} \\ u'_{m-3,n} \\ u'_{m-4,n} \\ u'_{m-5,n} \\ u'_{m-6,n} \\ u'_{m,n} \end{bmatrix}$$

$$A^{-1}D_M = \begin{bmatrix} 0 & 0 & 0 & 0 & 0 & 0 & \frac{416,173}{1,814,400} \\ 0 & 0 & 0 & 0 & 0 & 0 & \frac{14,939}{28,350} \\ 0 & 0 & 0 & 0 & 0 & 0 & \frac{18,399}{22,400} \\ 0 & 0 & 0 & 0 & 0 & 0 & \frac{15,824}{14,175} \\ 0 & 0 & 0 & 0 & 0 & 0 & \frac{102,425}{72,576} \\ 0 & 0 & 0 & 0 & 0 & 0 & \frac{597}{350} \\ 0 & 0 & 0 & 0 & 0 & 0 & \frac{519,253}{259,200} \end{bmatrix}, R_2 = \begin{bmatrix} f_{m-1,n} \\ f_{m-2,n} \\ f_{m-3,n} \\ f_{m-4,n} \\ f_{m-5,n} \\ f_{m-6,n} \\ f_{m,n} \end{bmatrix}$$

$$A^{-1}E_M = \begin{bmatrix} \frac{33,953}{64,800} & -\frac{341,699}{604,800} & \frac{105,943}{181,440} & -\frac{153,761}{362,880} & \frac{943}{4725} & -\frac{99,359}{1,814,400} & \frac{6031}{907,200} \\ \frac{27821}{14175} & -\frac{833}{675} & \frac{799}{567} & -\frac{5881}{5670} & \frac{2321}{4725} & -\frac{1916}{14,175} & \frac{233}{14,175} \\ \frac{39,141}{11,200} & -\frac{24,111}{22,400} & \frac{369}{160} & -\frac{7299}{4480} & \frac{8613}{11,200} & -\frac{4737}{22,400} & \frac{9}{350} \\ \frac{71,152}{14,175} & -\frac{3832}{4725} & \frac{11,344}{2835} & -\frac{856}{405} & \frac{4912}{4725} & -\frac{4072}{14,175} & \frac{496}{14,175} \\ \frac{59,375}{9072} & -\frac{13,375}{24,192} & \frac{21,0625}{36,288} & -\frac{130,625}{72,576} & \frac{1225}{864} & -\frac{26,875}{72,576} & \frac{1625}{36,288} \\ \frac{1413}{175} & -\frac{54}{175} & \frac{267}{35} & -\frac{99}{70} & \frac{459}{175} & -\frac{9}{25} & \frac{9}{175} \\ \frac{1,241,317}{129,600} & \frac{2401}{86,400} & \frac{12,005}{1296} & -\frac{40,817}{51,840} & \frac{160,867}{43,200} & \frac{146,461}{259,200} & \frac{8183}{64,800} \end{bmatrix}, R_3 = \begin{bmatrix} f_{m+1,n} \\ f_{m+2,n} \\ f_{m+3,n} \\ f_{m+4,n} \\ f_{m+5,n} \\ f_{m+6,n} \\ f_{m+7,n} \end{bmatrix}$$

The matrix Equation (12) can be written explicitly as follows

$$\begin{aligned} u_{m+1,n} = & u_{m,n} + u'_{m,n}h + \frac{416,173}{1,814,400} h^2 f_{m,n} + \frac{33,953}{64,800} h^2 f_{m+1,n} - \frac{341,699}{604,800} h^2 f_{m+2,n} \\ & + \frac{105,943}{181,440} h^2 f_{m+3,n} - \frac{153,761}{362,880} h^2 f_{m+4,n} + \frac{943}{4725} h^2 f_{m+5,n} - \frac{99,359}{1,814,400} h^2 f_{m+6,n} \\ & + \frac{6031}{907,200} h^2 f_{m+7,n}, \end{aligned} \quad (13)$$

$$\begin{aligned} u_{m+2,n} = & u_{m,n} + 2hu'_{m,n} + \frac{14,939}{28,350} h^2 f_{m,n} + \frac{27,821}{14,175} h^2 f_{m+1,n} - \frac{833}{675} h^2 f_{m+2,n} \\ & + \frac{799}{567} h^2 f_{m+3,n} - \frac{5881}{5670} h^2 f_{m+4,n} + \frac{2321}{4725} h^2 f_{m+5,n} - \frac{1916}{14,175} h^2 f_{m+6,n} \\ & + \frac{233}{14,175} h^2 f_{m+7,n}, \end{aligned} \quad (14)$$

$$\begin{aligned} u_{m+3,n} = & u_{m,n} + 3hu'_{m,n} + \frac{18,399}{22,400} h^2 f_{m,n} + \frac{39,141}{11,200} h^2 f_{m+1,n} - \frac{24,111}{22,400} h^2 f_{m+2,n} \\ & + \frac{369}{160} h^2 f_{m+3,n} - \frac{7299}{4480} h^2 f_{m+4,n} + \frac{8613}{11,200} h^2 f_{m+5,n} - \frac{4737}{22,400} h^2 f_{m+6,n} \\ & + \frac{9}{350} h^2 f_{m+7,n}, \end{aligned} \quad (15)$$

$$\begin{aligned}
u_{m+4,n} = & u_{m,n} + 4hu'_{m,n} + \frac{15,824}{14,175} h^2 f_{m,n} + \frac{71,152}{14,175} h^2 f_{m+1,n} - \frac{3832}{4725} h^2 f_{m+2,n} \\
& + \frac{11,344}{2835} h^2 f_{m+3,n} - \frac{856}{405} h^2 f_{m+4,n} + \frac{4912}{4725} h^2 f_{m+5,n} - \frac{4072}{14,175} h^2 f_{m+6,n} \\
& + \frac{496}{14,175} h^2 f_{m+7,n},
\end{aligned} \quad (16)$$

$$\begin{aligned}
u_{m+5,n} = & u_{m,n} + 5hu'_{m,n} + \frac{102,425}{72,576} h^2 f_{m,n} + \frac{59,375}{9072} h^2 f_{m+1,n} - \frac{13,375}{24,192} h^2 f_{m+2,n} \\
& + \frac{210,625}{36,288} h^2 f_{m+3,n} - \frac{130,625}{72,576} h^2 f_{m+4,n} + \frac{1225}{864} h^2 f_{m+5,n} - \frac{26,875}{72,576} h^2 f_{m+6,n} \\
& + \frac{1625}{36,288} h^2 f_{m+7,n},
\end{aligned} \quad (17)$$

$$\begin{aligned}
u_{m+6,n} = & u_{m,n} + 6hu'_{m,n} + \frac{597}{350} h^2 f_{m,n} + \frac{1413}{175} h^2 f_{m+1,n} - \frac{54}{175} h^2 f_{m+2,n} \\
& + \frac{267}{35} h^2 f_{m+3,n} - \frac{99}{70} h^2 f_{m+4,n} + \frac{459}{175} h^2 f_{m+5,n} - \frac{9}{25} h^2 f_{m+6,n} \\
& + \frac{9}{175} h^2 f_{m+7,n},
\end{aligned} \quad (18)$$

$$\begin{aligned}
u_{m+7,n} = & u_{m,n} + 7hu'_{m,n} + \frac{519,253}{259,200} h^2 f_{m,n} + \frac{1,241,317}{129,600} h^2 f_{m+1,n} + \frac{2401}{86,400} h^2 f_{m+2,n} \\
& + \frac{12,005}{1296} h^2 f_{m+3,n} - \frac{40,817}{51,840} h^2 f_{m+4,n} + \frac{160,867}{43,200} h^2 f_{m+5,n} + \frac{146,461}{259,200} h^2 f_{m+6,n} \\
& + \frac{8183}{64,800} h^2 f_{m+7,n}
\end{aligned} \quad (19)$$

with the corresponding first derivatives

$$\begin{aligned}
u'_{m+1,n} = & u'_{m,n} + \frac{5257}{17,280} h f_{m,n} + \frac{139,849}{120,960} h f_{m+1,n} - \frac{4511}{4480} h f_{m+2,n} + \frac{123,133}{120,960} h f_{m+3,n} \\
& - \frac{88,547}{120,960} h f_{m+4,n} + \frac{1537}{4480} h f_{m+5,n} - \frac{11,351}{120,960} h f_{m+6,n} + \frac{275}{24,192} h f_{m+7,n},
\end{aligned} \quad (20)$$

$$\begin{aligned}
u'_{m+2,n} = & u'_{m,n} + \frac{41}{140} h f_{m,n} + \frac{1466}{945} h f_{m+1,n} - \frac{71}{420} h f_{m+2,n} + \frac{68}{105} h f_{m+3,n} \\
& - \frac{1927}{3780} h f_{m+4,n} + \frac{26}{105} h f_{m+5,n} - \frac{29}{420} h f_{m+6,n} + \frac{8}{945} h f_{m+7,n},
\end{aligned} \quad (21)$$

$$\begin{aligned}
u'_{m+3,n} = & u'_{m,n} + \frac{265}{896} h f_{m,n} + \frac{1359}{896} h f_{m+1,n} + \frac{1377}{4480} h f_{m+2,n} + \frac{5927}{4480} h f_{m+3,n} \\
& - \frac{3033}{4480} h f_{m+4,n} + \frac{1377}{4480} h f_{m+5,n} - \frac{373}{4480} h f_{m+6,n} + \frac{9}{896} h f_{m+7,n},
\end{aligned} \quad (22)$$

$$\begin{aligned}
u'_{m+4,n} = & u'_{m,n} + \frac{278}{945} h f_{m,n} + \frac{1448}{945} h f_{m+1,n} + \frac{8}{35} h f_{m+2,n} + \frac{1784}{945} h f_{m+3,n} \\
& - \frac{106}{945} h f_{m+4,n} + \frac{8}{35} h f_{m+5,n} - \frac{64}{945} h f_{m+6,n} + \frac{8}{945} h f_{m+7,n},
\end{aligned} \quad (23)$$

$$u'_{m+5,n} = u'_{m,n} + \frac{265}{896} hf_{m,n} + \frac{36,725}{24,192} hf_{m+1,n} + \frac{775}{2688} hf_{m+2,n} + \frac{4625}{2688} hf_{m+3,n} \quad (24)$$

$$+ \frac{13,625}{24,192} hf_{m+4,n} + \frac{1895}{2688} hf_{m+5,n} - \frac{275}{2688} hf_{m+6,n} + \frac{275}{24,192} hf_{m+7,n},$$

$$u'_{m+6,n} = u'_{m,n} + \frac{41}{140} hf_{m,n} + \frac{54}{35} hf_{m+1,n} + \frac{27}{140} hf_{m+2,n} + \frac{68}{35} hf_{m+3,n} \quad (25)$$

$$+ \frac{27}{140} hf_{m+4,n} + \frac{54}{35} hf_{m+5,n} + \frac{41}{140} hf_{m+6,n} + 0 hf_{m+7,n},$$

$$u'_{m+7,n} = u'_{m,n} + \frac{5257}{17,280} hf_{m,n} + \frac{25,039}{17,280} hf_{m+1,n} + \frac{343}{640} hf_{m+2,n} + \frac{20,923}{17,280} hf_{m+3,n} \quad (26)$$

$$+ \frac{20,923}{17,280} hf_{m+4,n} + \frac{343}{640} hf_{m+5,n} + \frac{25,039}{17,280} hf_{m+6,n} + \frac{5257}{17,280} hf_{m+7,n}$$

Remark 1. The integrators (13)–(26) formed the HFBI needed for the implementation of the resulting second-order system of ODEs emerging from the discretization of the PDEs of the form (1).

3. Basic Properties of the HFBI

3.1. Order and Error Terms of the HFBI

The basic properties of the HFBI such as the local truncation error (LTE), order and error terms, zero-stability, and stability nature are investigated in the spirit of Lambert [33] and Henrici [34].

The local truncation error (LTE) of HFBI is expressed by

$$L[u(x); h] = u(x + jh, t) - \sum_{j=0}^{\rho} [\gamma_j u(x + jh, t)] - h^2 \sum_{j=0}^{\mu} [\psi_j u''(x + jh, t)], \quad (27)$$

where $u(x)$ is continuously differentiable, $\rho = 1$, $\mu = 7$ and $j = 0(1)7$.

Expanding $u(x + jh, t)$ and $u''(x + jh, t)$ in (27) in the Taylor series about x_n , and collecting the like terms in h and y yields,

$$L[u(x); h] = F_0 u(x) + F_1 h u'(x) + F_2 h^2 u''(x) + \dots + F_q h^q u^{(q)}(x) \quad (28)$$

where $F_q, q = 1, 2, \dots$ are given as follows:

$$F_0 = \sum_{j=0}^k \gamma_j$$

$$F_1 = \sum_{j=0}^k j \gamma_j - \sum_{j=0}^k \psi_j$$

$$F_2 = \frac{1}{2!} \sum_{j=0}^k j^2 \gamma_j - \left(\sum_{j=0}^k j \psi_j \right) \quad (29)$$

$$F_3 = \frac{1}{3!} \sum_{j=0}^k j^3 \gamma_j - \left(\sum_{j=0}^k j^2 \psi_j \right)$$

$$\vdots$$

$$\vdots$$

$$\vdots$$

$$F_q = \frac{1}{q!} \sum_{j=0}^k j^q \gamma_j - q \left(\sum_{j=0}^k j^{q-1} \psi_j \right)$$

Thus, the method is of order p if $F_0 = F_1 = \dots = F_p = 0, F_{p+2} \neq 0$.

Hence, F_{p+2} is the error constant, and F'_i s are the error constants.

The local truncation error (LTE) is given by

$$(LTE) = F_{p+2} h^{p+2} u^{(p+2)}(x_n) + O(h^{(p+3)}) \quad (30)$$

Remark 2. The method (13)–(26) is of order p if $F_0 = F_1 = \dots = F_{p+1} = 0$, and $F_{p+2} \neq 0$.

3.2. Zero-Stability of the HFBI

The matrix difference Equation (12) is given by

$$A^{(0)}U_w = A^{(1)}U_{w-1} + h^2 \left[B^{(0)}F_w + B^{(1)}F_{w-1} \right] \quad (31)$$

It should be noted that the matrices $A^{(0)}$, $A^{(1)}$, $B^{(0)}$ and $B^{(1)}$ are square matrices whose entries are the coefficients of (13)–(19) above and are defined as follows:

$$A^{(0)} = \begin{bmatrix} 1 & 0 & 0 & 0 & 0 & 0 & 0 \\ 0 & 1 & 0 & 0 & 0 & 0 & 0 \\ 0 & 0 & 1 & 0 & 0 & 0 & 0 \\ 0 & 0 & 0 & 1 & 0 & 0 & 0 \\ 0 & 0 & 0 & 0 & 1 & 0 & 0 \\ 0 & 0 & 0 & 0 & 0 & 1 & 0 \\ 0 & 0 & 0 & 0 & 0 & 0 & 1 \end{bmatrix}, A^{(1)} = \begin{bmatrix} 0 & 0 & 0 & 0 & 0 & 0 & 1 \\ 0 & 0 & 0 & 0 & 0 & 0 & 1 \\ 0 & 0 & 0 & 0 & 0 & 0 & 1 \\ 0 & 0 & 0 & 0 & 0 & 0 & 1 \\ 0 & 0 & 0 & 0 & 0 & 0 & 1 \\ 0 & 0 & 0 & 0 & 0 & 0 & 1 \\ 0 & 0 & 0 & 0 & 0 & 0 & 1 \end{bmatrix}$$

$$B^{(0)} = \begin{bmatrix} \frac{33,953}{64,800} & -\frac{341,699}{604,800} & \frac{105,943}{181,440} & -\frac{153,761}{362,880} & \frac{943}{4725} & -\frac{99,359}{1,814,400} & \frac{6031}{907,200} \\ \frac{27,821}{14,175} & -\frac{833}{675} & \frac{799}{567} & -\frac{5881}{5670} & \frac{2321}{4725} & -\frac{1916}{14,175} & \frac{233}{14,175} \\ \frac{39,141}{11,200} & -\frac{24,111}{22,400} & \frac{369}{160} & -\frac{7299}{4480} & \frac{8613}{11,200} & -\frac{4737}{22,400} & \frac{9}{350} \\ \frac{71,152}{14,175} & -\frac{3832}{4725} & \frac{11,344}{2835} & -\frac{856}{405} & \frac{4912}{4725} & -\frac{4072}{14,175} & \frac{496}{14,175} \\ \frac{59,375}{9072} & -\frac{13,375}{24,192} & \frac{210,625}{36,288} & -\frac{130,625}{72,576} & \frac{1225}{864} & -\frac{26,875}{72,576} & \frac{1625}{36,288} \\ \frac{1413}{175} & -\frac{54}{175} & \frac{267}{35} & -\frac{99}{70} & \frac{459}{175} & -\frac{9}{25} & \frac{9}{175} \\ \frac{1,241,317}{129,600} & \frac{2401}{86,400} & \frac{12,005}{1296} & -\frac{40,817}{51,840} & \frac{160,867}{43,200} & \frac{146,461}{259,200} & \frac{8183}{64,800} \end{bmatrix}$$

$$B^{(1)} = \begin{bmatrix} 0 & 0 & 0 & 0 & 0 & 0 & \frac{416,173}{1,814,400} \\ 0 & 0 & 0 & 0 & 0 & 0 & \frac{14,939}{28,350} \\ 0 & 0 & 0 & 0 & 0 & 0 & \frac{18,399}{22,400} \\ 0 & 0 & 0 & 0 & 0 & 0 & \frac{15,824}{14,175} \\ 0 & 0 & 0 & 0 & 0 & 0 & \frac{102,425}{72,576} \\ 0 & 0 & 0 & 0 & 0 & 0 & \frac{597}{350} \\ 0 & 0 & 0 & 0 & 0 & 0 & \frac{519,253}{259,200} \end{bmatrix}$$

$$U_w = \left[u_{m+1,n}, u_{m+2,n}, u_{m+3,n}, u_{m+4,n}, u_{m+5,n}, u_{m+6,n}, u_{m+7,n} \right]^T$$

$$U_{w-1} = \left[u_{m-6,n}, u_{m-5,n}, u_{m-4,n}, u_{m-3,n}, u_{m-2,n}, u_{m-1,n}, u_{m,n} \right]^T$$

$$F_w = \left[f_{m+1,n}, f_{m+2,n}, f_{m+3,n}, f_{m+4,n}, f_{m+5,n}, f_{m+6,n}, f_{m+7,n} \right]^T$$

$$F_{w-1} = \left[f_{m-6,n}, f_{m-5,n}, f_{m-4,n}, f_{m-3,n}, f_{m-2,n}, f_{m-1,n}, f_{m,n} \right]^T$$

The zero-stability is concerned with the stability of the different systems in the limit as h tends to 0 in (12). Consequently, as h tends 0, the method (31) tends to the different system.

$$A^{(0)}U_w - A^{(1)}U_{w-1} = 0 \quad (32)$$

The first characteristics of (32) is given by

$$\rho(R) = \det(RA^{(0)} - A^{(1)}) = 0 \quad (33)$$

$$\det[RA^{(0)} - A^{(1)}] = 0 \quad (34)$$

According to Fatunla [36], the new method, HFBI is said to be zero-stable if (34) holds, then

$$\rho(R) = R^6(R - 1) = R_1 = R_2 = R_3 = R_4 = 0 = R_5 = 0, R_6 = 0, R = 1 \quad (35)$$

Hence, the new method, HFBI, is zero-stable [34].

3.3. Consistency

As stated by Lambert in [33], the methods (13)–(19) are consistent if they have order p greater than or equal to 1. Hence, the method is consistent, since (13)–(19) have order $p = 8 > 1$ (see the details in Table 1). hence it is consistent.

Table 1. Analysis of the order and error constant of HFBI in (13)–(26).

Equation	Formulae	Error Constant	Order p
13	$u_{m+1,n}$	-5.537230×10^{-3}	8
14	$u_{m+2,n}$	-1.378307×10^{-2}	8
15	$u_{m+3,n}$	-2.159598×10^{-2}	8
16	$u_{m+4,n}$	-2.948854×10^{-2}	8
17	$u_{m+5,n}$	-3.746073×10^{-2}	8
18	$u_{m+6,n}$	-4.500000×10^{-2}	8
19	$u_{m+7,n}$	-5.524788×10^{-2}	8
20	$u'_{m+1,n}$	-9.356537×10^{-3}	8
21	$u'_{m+2,n}$	-7.345679×10^{-3}	8
22	$u'_{m+3,n}$	-8.236607×10^{-3}	8
23	$u'_{m+4,n}$	-7.548501×10^{-3}	8
24	$u'_{m+5,n}$	-8.439429×10^{-3}	8
25	$u'_{m+6,n}$	-6.428571×10^{-3}	8
26	$u'_{m+7,n}$	-1.578511×10^{-2}	8

3.4. Convergence

The method (13)–(19) is in the form of general linear multistep method. It is very important that the method be consistent and zero-stable. The method is convergent since it satisfied the conditions for consistency and zero-stability as established by [34].

3.5. Region of Absolute Stability of HFBI

The region of absolute stability of the HFBI was investigated via the procedure discussed in [33,37]. The stability matrix can be expressed as

$$M(z) = zS(I - zW)^{-1}U + V \quad (36)$$

together with the stability function

$$p(n, z) = \det(-M(z) + nI) \quad (37)$$

For the stability properties, the integrator (13)–(19) was formulated as a general linear method of the form:

$$\begin{bmatrix} Y \\ \vdots \\ Y_{i+1} \end{bmatrix} = \begin{bmatrix} W & & U \\ & \ddots & \\ S & & V \end{bmatrix} \begin{bmatrix} h^2 f(u) \\ \vdots \\ Y_{i-1} \end{bmatrix} \quad (38)$$

where n represents the roots of the first characteristic polynomial of the method (12), and

$$Y_{i-1} = \begin{bmatrix} u_{m+1,n} \\ u_{m,n} \end{bmatrix}, Y_{i+1} = \begin{bmatrix} u_{m+1,n} \\ u_{m+7,n} \end{bmatrix},$$

$$W = \begin{bmatrix} 0 & 0 & 0 & 0 & 0 & 0 & 0 & 0 \\ \frac{416,173}{1,814,400} & \frac{33,953}{64,800} & -\frac{341,699}{604,800} & \frac{105,943}{181,440} & -\frac{153,761}{362,880} & \frac{943}{4725} & -\frac{99,359}{1,814,400} & \frac{6031}{907,200} \\ \frac{14,939}{28,350} & \frac{27,821}{14,175} & -\frac{833}{675} & \frac{799}{567} & -\frac{5881}{5670} & \frac{2321}{4725} & -\frac{1916}{14,175} & \frac{233}{14,175} \\ \frac{18,399}{22,400} & \frac{39,141}{11,200} & -\frac{24,111}{22,400} & \frac{369}{160} & -\frac{7299}{4480} & \frac{8613}{11,200} & -\frac{4737}{22,400} & \frac{9}{350} \\ \frac{15,824}{14,175} & \frac{71,152}{14,175} & -\frac{3832}{4725} & \frac{11,344}{2835} & -\frac{856}{405} & \frac{4912}{4725} & -\frac{4072}{14,175} & \frac{496}{14,175} \\ \frac{102,425}{72,576} & \frac{59,375}{9072} & -\frac{13,375}{24,192} & \frac{210,625}{36,288} & -\frac{130,625}{72,576} & \frac{1225}{864} & -\frac{26,875}{72,576} & \frac{1625}{36,288} \\ \frac{597}{350} & \frac{1413}{175} & -\frac{54}{175} & \frac{267}{35} & -\frac{99}{70} & \frac{459}{175} & -\frac{9}{25} & \frac{9}{175} \\ \frac{519,253}{259,200} & \frac{1,241,317}{129,600} & \frac{2401}{86,400} & \frac{12,005}{1296} & -\frac{40,817}{51,840} & \frac{160,867}{43,200} & \frac{146,461}{259,200} & \frac{8183}{64,800} \end{bmatrix}$$

$$S = \begin{bmatrix} \frac{416,173}{1,814,400} & \frac{33,953}{64,800} & -\frac{341,699}{604,800} & \frac{105,943}{181,440} & -\frac{153,761}{362,880} & \frac{943}{4725} & -\frac{99,359}{1,814,400} & \frac{6031}{907,200} \\ \frac{519,253}{259,200} & \frac{1,241,317}{129,600} & \frac{2401}{86,400} & \frac{12,005}{1296} & -\frac{40,817}{51,840} & \frac{160,867}{43,200} & \frac{146,461}{259,200} & \frac{8183}{64,800} \end{bmatrix}$$

$$V = \begin{bmatrix} 0 & 1 \\ 0 & 1 \end{bmatrix}, U = \begin{bmatrix} 0 & 1 \\ 0 & 1 \\ 0 & 1 \\ 0 & 1 \\ 0 & 1 \\ 0 & 1 \\ 0 & 1 \end{bmatrix}, Y = \begin{bmatrix} u_{m+1,n} \\ u_{m+2,n} \\ u_{m+3,n} \\ u_{m+4,n} \\ u_{m+5,n} \\ u_{m+6,n} \\ u_{m+7,n} \end{bmatrix}, I = \begin{bmatrix} 1 & 0 \\ 0 & 1 \end{bmatrix}, f(u) = \begin{bmatrix} f_{m+1,n} \\ f_{m+2,n} \\ f_{m+3,n} \\ f_{m+4,n} \\ f_{m+5,n} \\ f_{m+6,n} \\ f_{m+7,n} \end{bmatrix}$$

Now, putting the values of the variables W, S, U, V, M and I into Equations (36) and (37), we obtained the stability function. The stability function and its derivatives were then plotted in the MATLAB (R2012a) environment. It should be noted that M is 8 by 8 identity matrix. The region of absolute stability (RAS) of the HFBI is displayed in the Figure 1 below,

Definition 1. The method of the class (13)–(26) is said to be p -stable if its interval of periodicity lies within $(0, \infty)$. The interval of periodicity of the HFBI lies within $(0, 0.091)$ as ascertained in Figure 1, which shows that the method is p -stable (see [33]).

The shaded portion inside the curve indicates the unstable region, while the external region outside the curve represents the stable region [26].

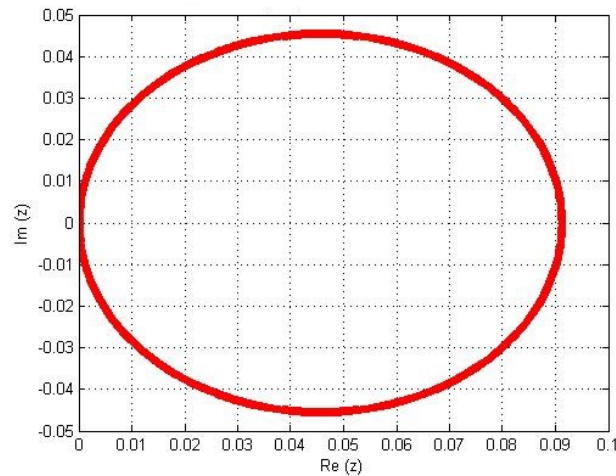


Figure 1. RAS of HFBI.

4. Computational Approach

The method of lines is a very powerful tool for transforming PDEs into ODEs [38]. In this section, the procedures for the discretization of second-order anisotropic elliptic partial differential equations into systems of second-order ordinary differential equations via the MOL approach are illustrated. We applied MOL to transform (1) to a system of second-order ODEs with the initial conditions in the form below. In particular, the y variable was discretized with the mesh spacings,

$$\Delta x = \frac{b-a}{M}, \quad x_i = a + i\Delta x, \quad i = 0, 1, \dots, M. \quad (39)$$

For each $i = 0, \dots, M$ and for a fixed y in $[a, b]$, we define:

$$\Delta t = \frac{d-c}{N}, \quad t_i = c + i\Delta t, \quad i = 0, 1, \dots, N. \quad (40)$$

For each $i = 0, \dots, N$ and for a fixed t in $[c, d]$,

The following vectors are defined

$$u_i(y) \cong u(x_i, y), \quad u(y) = [u_0(y), u_1(y), u_2(y), \dots, u_M(y)]^T, \\ f_i(y) \cong f(x_i, y), \quad f(y) = [f_0(y), f_1(y), f_2(y), \dots, f_M(y)]^T,$$

In addition, the partial derivatives $\frac{\partial^2 u}{\partial y^2}$ appearing in (1) are replaced by the second-order central difference approximations

$$\frac{\partial^2 u}{\partial y^2} = \frac{u(x, y_{m+1}) - 2u(x, y_m) + u(x, y_{m-1}, y)}{(\Delta y)^2}, \quad m = 1, \dots, M-1. \quad (41)$$

Hence, problem (1) has the following semi-discretized form given below;

$$\frac{d^2 u_{m,n}}{dx^2} = - \left[\frac{u(x, y_{m+1}) - 2u(x, y_m) + u(x, y_{m-1}, y)}{(\Delta y)^2} \right] + g_{m,n} \quad (42)$$

which could also be written in the form

$$\mathbf{u}'' = \mathbf{f}(x, \mathbf{u}, \mathbf{u}') = T\mathbf{u} + \mathbf{g}, \quad (43)$$

subject to the initial conditions

$$\mathbf{u}(a) = \mathbf{u}_0, \quad \mathbf{u}'(a) = \mathbf{u}'_0, \quad (44)$$

or any of the boundary conditions

$$\mathbf{u}(a) = \mathbf{u}_0, \quad \mathbf{u}'(a) = \mathbf{u}'_{m,n}, \quad (45)$$

$$\mathbf{u}'(b) = \mathbf{u}'_0, \quad \mathbf{u}'(c) = \mathbf{u}'_{m,n}. \quad (46)$$

T is the tridiagonal matrix given as

$$T = \begin{pmatrix} \frac{-2}{(\Delta y)^2} & \frac{1}{(\Delta y)^2} & 0 & \cdots & \cdots & 0 & 0 & 0 \\ \frac{1}{(\Delta y)^2} & \frac{-2}{(\Delta y)^2} & \frac{1}{(\Delta y)^2} & \cdots & \cdots & 0 & 0 & 0 \\ 0 & \frac{1}{(\Delta y)^2} & \frac{-2}{(\Delta y)^2} & \cdots & \cdots & 0 & 0 & 0 \\ \vdots & \vdots & \vdots & \vdots & \cdots & \vdots & \cdots & \cdots \\ \vdots & \vdots & \vdots & \vdots & \cdots & \vdots & \cdots & \cdots \\ 0 & 0 & 0 & \cdots & \cdots & \frac{-2}{(\Delta y)^2} & \frac{1}{(\Delta y)^2} & 0 \\ 0 & 0 & 0 & \cdots & \vdots & \frac{1}{(\Delta y)^2} & \frac{-2}{(\Delta y)^2} & \frac{1}{(\Delta y)^2} \\ 0 & 0 & 0 & \vdots & \cdots & 0 & \frac{1}{(\Delta y)^2} & \frac{-2}{(\Delta y)^2} \end{pmatrix}$$

$U = [u, u']^T$ and g is a vector of constants.

The resulting equation arising from the semi-discretized Equation (42) which is expressed in form (43) and solved by the HFBI.

5. Numerical Examples

The accuracy and efficiency of the HFBI are shown in this section. Three numerical examples of anisotropic elliptic second-order partial differential models sourced from the recent literature were executed using a written program in Mathematica [11.0]. The computational results obtained by the HFBI were investigated in comparison with the existing methods in the literature. The results are presented in tabular form to show the superiority of HFBI in terms of accuracy and efficiency.

The absolute error (AE) is given by $AE = \max |u(x_m, t_m) - u_m(t_n)|$.

It follows that $u(x_m, t_m)$ is the exact solution, and $u_m(t_n)$ is the approximate solution at the mesh point (x_m, t_m) .

Example 1. The first second-order anisotropic elliptic PDEs are taken from [39]

$$\frac{\partial^2 u}{\partial x^2}(x, y) + \frac{\partial^2 u}{\partial y^2}(x, y) = -2\pi^2 \sin(\pi x) \cos(\pi y), \quad \text{for } 0 \leq x \leq 1, \quad 0 \leq y \leq 1 \quad (47)$$

with the conditions below

$$\begin{aligned} u(0, y) &= 0, \\ u(x, 0) &= \sin(\pi x), \\ u(1, y) &= 0, \\ u(x, 1) &= -\sin(\pi x) \end{aligned} \quad (48)$$

The theoretical solution of (47) is given as

$$u(x, y) = \sin(\pi x) \cos(\pi y) \quad (49)$$

We compared the numerical results of the HFBI with the exact solution (49) and the absolute error obtained is also presented. In Table 2, the exact solution, computed solution, and the absolute error for Example 1 are displayed in column 1, column 2, and column 3, respectively. It can be seen that the results of the computed solution were in good agreement or very close to the exact solution. This shows that the method contained a high rate of convergence. In other to access the accuracy of the HFBI, we compared with other researchers in the literature who have also solved the problem namely Wang & Zhang [39] which is denoted with WZ09 and Sun & Zhang [28] represented with SZ04 in Figure 2.

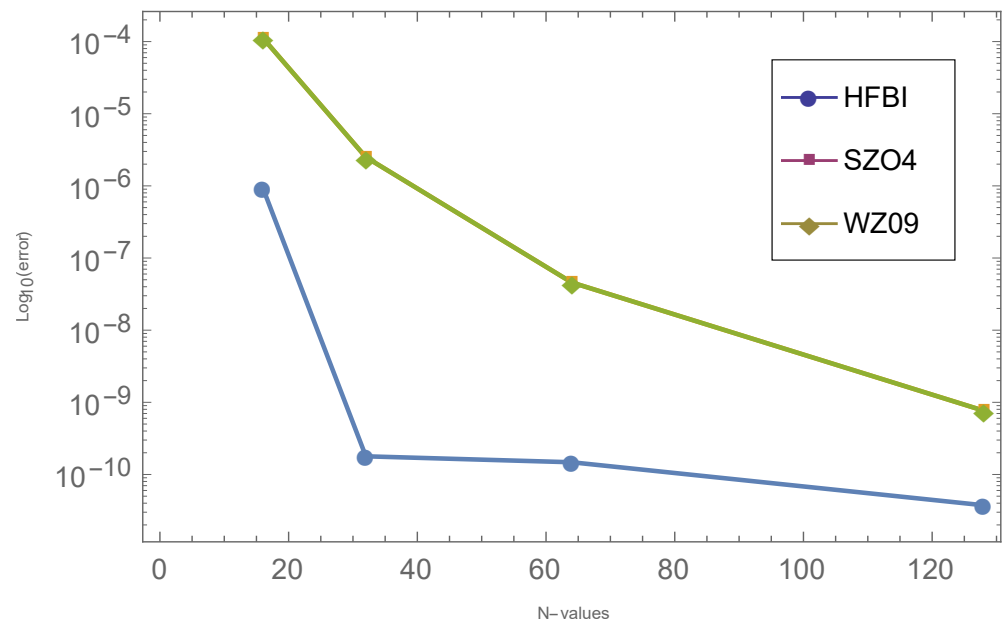


Figure 2. Efficiency curve for Problem 1.

Table 2. Numerical results of exact-solution, computed-solution, and the Absolute error in HFBI for Problem 2.

N	Exact-Solution	Computed-Solution	AE in HFBI
2	0.950651965960978000	0.951056516295153500	4.045503×10^{-4}
4	0.703696743499951600	0.703701868763191200	5.125263×10^{-6}
8	0.380836408840172200	0.380840707040230040	4.298200×10^{-6}
16	0.194151840094070400	0.194150908792011470	9.313021×10^{-7}
32	0.098009759640639170	0.098009759819161480	1.785223×10^{-10}
64	0.049063979474120880	0.049063979621783700	1.476628×10^{-10}
128	0.024539380650971644	0.024539380613539380	3.743227×10^{-11}

Wang & Zhang in [39] proposed an algorithm entitled a sixth-order compact scheme combined with multigrid method and extrapolation technique, while Sun & Zhang in [28] developed a method titled a high-order finite difference discretization strategy based on extrapolation. In Table 3, we present the comparison of the absolute error in the HFBI, Wang & Zhang in [39] and Sun & Zhang in [28] with N varying from $N = 2, 4, 8, 16, 32, 64$ and 128. It is obvious that generally as N increased, the accuracies also increased. The accuracy also decreased as N decreased. The HFBI performed better than Wang & Zhang [39] which is denoted with WZ09 and Sun & Zhang [28] represented with SZ04 in Figure 2 in terms of convergence and accuracy.

Table 3. Comparison of AE in HFBI with [39] and AE in [28] for Problem 1.

N	AE in HFBI	AE in [39]	AE in [28]
2	4.045503×10^{-4}	—	—
4	5.125263×10^{-6}	—	—
8	4.298200×10^{-6}	—	—
16	9.313021×10^{-7}	1.12×10^{-4}	1.12×10^{-4}
32	1.785223×10^{-10}	2.50×10^{-6}	2.50×10^{-6}
64	1.476628×10^{-10}	4.58×10^{-8}	4.58×10^{-8}
128	3.743227×10^{-11}	7.66×10^{-10}	7.66×10^{-10}

Remark 3. - means Not Available.

Example 2. Next, we take the following anisotropic equation solved by [30]

$$\frac{\partial^2 u}{\partial x^2}(x, y) + \frac{\partial^2 u}{\partial y^2}(x, y) - \sin(\pi x) \sin(\pi y), \quad 0 < x, y < 1, \quad (50)$$

subjected to the following conditions

$$\begin{aligned} u(x, 0) = 0, u(0, y) = 0, u(x, 1) = 0, u(1, y) = 0 \\ \frac{\partial u}{\partial x}(0, y) = -\frac{\sin(\pi y)}{2\pi}, \frac{\partial u}{\partial x}(x, 0) = 0, \frac{\partial u}{\partial y}(0, x) = 0, \frac{\partial u}{\partial y}(x, 0) = -\frac{\sin(\pi x)}{2\pi} \\ \frac{\partial u}{\partial x}(1, y) = \frac{\sin(\pi y)}{2\pi}, \frac{\partial u}{\partial y}(x, 1) = 0, \frac{\partial u}{\partial y}(1, y) = 0, \frac{\partial u}{\partial x}(x, 1) = \frac{\sin(\pi x)}{2\pi} \end{aligned} \quad (51)$$

The theoretical solution of (50) is given as

$$u(x, y) = -\frac{\sin(\pi x) \sin(\pi y)}{2\pi^2} \quad (52)$$

Now, in Table 4, The numerical computation of the HFBI for problem (50) is presented. Furthermore, the comparison of the absolute error in HFBI is made with Raslan et al. [30], as shown in Table 5. In their article, they proposed an extended cubic B-splines by Raslan et al. in [30] which is denoted with RA21 in Figure 3. The accuracy of the HFBI over Raslan et al. in [30] is also demonstrated in Table 5 and the efficiency curve in Figure 3. Hence, the new method is superior to the existing method of Raslan et al. in [30].

Example 3. Finally, we take the following inhomogeneous elliptic equation studied by [40]

$$\nabla^2 u - 2u = -4(1-x)(1-y)(x+y)e^{-x-y}, \quad (x, y) \in R = (0, 1) \times (0, 1), \quad (53)$$

which is governed by the homogeneous boundary conditions $u = 0$ on ∂R .

The analytical smooth solution of (53) is given as

$$u(x, y) = xy(1-x)(1-y)e^{-x-y} \quad (54)$$

Remark 4. S3CPCM: Shifted Third-kind Chebyshev Petro-Galerkin method proposed by [40].
S4CPCM: Shifted Fourth-kind Chebyshev Petro-Galerkin method proposed by [40].
MAE: Maximum absolute error.

S3CPCM—Shifted Third-kind Chebyshev Petro-Galerkin method proposed by [40]

S4CPCM—Shifted Fourth-kind Chebyshev Petro-Galerkin method proposed by [40]

Ashry et al. in [40] proposed the Shifted Third-kind Chebyshev Petro-Galerkin method (S3CPCM) and Shifted Fourth-kind Chebyshev Petro-Galerkin method (S4CPCM) for the treatment of one- and two-dimensional second-order BVPs. The methods were also applied to solve an inhomogeneous elliptic equation. In Table 6, we compare the MAE of the HFBI with the S3CPCM and S4CPCM with $N = 3, 6$, and 9 . Figure 4 depicts the comparison

of the MAE in curves. Apparently, the HFBI showed some level of high accuracies with minimal error against Ashry et al. [40].

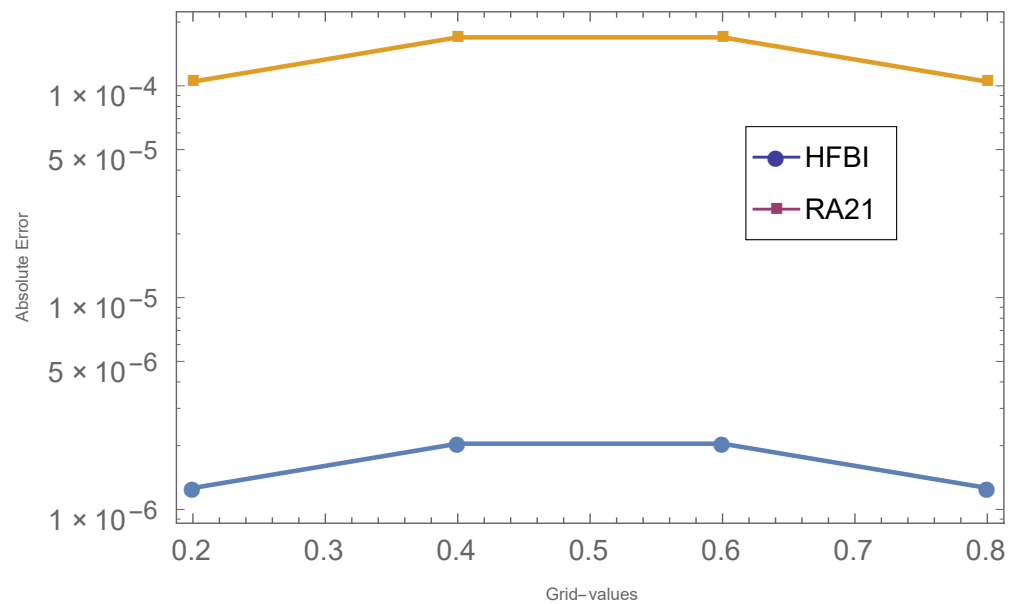


Figure 3. Efficiency curve for Problem 2.

Table 4. Numerical results of exact-solution, computed-solution and the Absolute error of the HFBI for Problem 2.

x	Exact-Solution	Computed-Solution	AE in HFBI
0.1	−0.004836992197904119	−0.004837656046375394	6.63848×10^{-7}
0.2	−0.009200505898171044	−0.009201768612999936	1.26271×10^{-6}
0.3	−0.012663409977431005	−0.01266514795529222	1.73798×10^{-6}
0.4	−0.014886731256934604	−0.014888774372445875	2.04312×10^{-6}
0.5	−0.015652835559053807	−0.015654983817833652	2.14826×10^{-6}
0.6	−0.014886731256934628	−0.014888774372445875	2.04312×10^{-6}
0.7	−0.012663409977431019	−0.01266514795529222	1.73798×10^{-6}
0.8	−0.009200505898171032	−0.00920176861299994	1.26271×10^{-6}
0.9	−0.004836992197904098	−0.004837656046375396	6.63848×10^{-7}

Table 5. Comparison of AE in HFBI with Extended Cubic B-Splines proposed by [30] for Problem 2.

x	AE in HFBI	AE in [30]
0.2	1.26271×10^{-6}	1.04701×10^{-4}
0.4	2.04312×10^{-6}	1.69408×10^{-4}
0.6	2.04312×10^{-6}	1.69408×10^{-4}
0.8	1.26271×10^{-6}	1.04701×10^{-4}

Table 6. Comparison of MAE in HFBI with MAE in S3CPCM and S4CPCM both proposed by [40] for Problem 3.

N	MAE in HFBI	MAE in S3CPCM [40]	MAE in S4CPCM [40]
3	1.60×10^{-8}	3.26×10^{-3}	4.11×10^{-3}
6	4.80×10^{-10}	2.53×10^{-5}	3.61×10^{-5}
9	6.34×10^{-11}	5.19×10^{-10}	7.46×10^{-10}

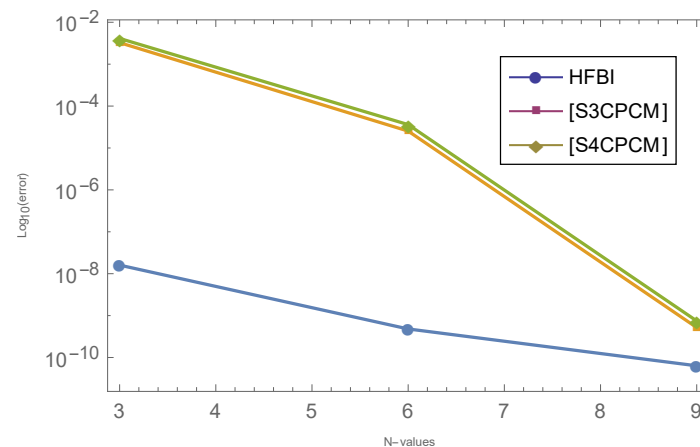


Figure 4. Efficiency curve for Problem 3.

6. Conclusions

In this study, we have successfully developed, analyzed, and implemented an HFBI. The derivation involved a Hermite polynomial as the basic function through the interpolation and collocation techniques. The HFBI of convergence order eight was zero-stable and consistent, and the region of absolute stability was examined through the boundary locus method and found to be absolutely-stable, as shown in Figure 1. The HFBI was applied to solve the resulting second-order ODEs arising from the semi-discretization of the second-order partial differential equations. Three test problems that have applications in physics and engineering were tested on the HFBI, and the results were presented in tabular form. The comparison of the computed solution and the exact solution was made in Tables 2 and 4 and also compared with existing methods in the recent literature in Tables 3, 5 and 6 for problems 1–3. The comparison of the HFBI in curves was also shown in Figures 2–4. Finally, the HFBI was in good agreement with the theoretical solution and compared favorably with the existing methods cited in the literature. The superiority of the results to other approaches shows that the application of Hermite polynomial as a basis function is a good candidate for such a class of problem [35]. The method is computationally reliable, accurate, and efficient.

Author Contributions: Funding acquisition, S.-W.Y.; Investigation, S.-W.Y.; Methodology, E.O.A., E.O.O. and A.S. All authors have read and agreed to the published version of the manuscript.

Funding: This research was funded by the National Natural Science Foundation of China (No. 71601072), the Fundamental Research Funds for the Universities of Henan Province (No. NSFRF210314), and the Innovative Research Team of Henan Polytechnic University (No. T2022-7).

Institutional Review Board Statement: Not applicable.

Informed Consent Statement: Not applicable.

Data Availability Statement: Not applicable.

Acknowledgments: The authors thank the anonymous referees whose suggestions helped improve this manuscript.

Conflicts of Interest: The authors declare no conflict of interest.

Appendix A

$$c_0 = u_{m,n},$$

$$c_1 = -\frac{1}{1,814,400h} (416,173 h^2 f_{m,n} + 950,684 h^2 f_{m+1,n} - 1,025,097 h^2 f_{m+2,n} \\ + 1,059,430 h^2 f_{m+3,n} - 768,805 h^2 f_{m+4,n} + 362,112 h^2 f_{m+5,n} - 99,359 h^2 f_{m+6,n} \\ + 12,062 h^2 f_{m+7,n} + 1,814,400 u_{m,n} - 1,814,400 u_{m+1,n}),$$

$$c_2 = \frac{1}{2} f_{m,n},$$

$$c_3 = -\frac{1}{2520h} (1089 f_{m,n} - 2940 f_{m+1,n} + 4410 f_{m+2,n} - 4900 f_{m+3,n} + 3675 f_{m+4,n} \\ - 1764 f_{m+5,n} + 490 f_{m+6,n} - 60 f_{m+7,n}),$$

$$c_4 = \frac{1}{4320h^2} (938 f_{m,n} - 4014 f_{m+1,n} + 7911 f_{m+2,n} - 9490 f_{m+3,n} + 7380 f_{m+4,n} \\ - 3618 f_{m+5,n} + 1019 f_{m+6,n} - 126 f_{m+7,n}),$$

$$c_5 = -\frac{1}{14,400h^3} (967 f_{m,n} - 5104 f_{m+1,n} + 11,787 f_{m+2,n} - 15,560 f_{m+3,n} + 12,725 f_{m+4,n} \\ - 6432 f_{m+5,n} + 1849 f_{m+6,n} - 232 f_{m+7,n}),$$

$$c_6 = -\frac{1}{4320h^4} (967 f_{m,n} - 5104 f_{m+1,n} + 11,787 f_{m+2,n} - 15,560 f_{m+3,n} + 12,725 f_{m+4,n} \\ - 6432 f_{m+5,n} + 1849 f_{m+6,n} - 232 f_{m+7,n}),$$

$$c_7 = -\frac{1}{30,240h^5} (46 f_{m,n} - 295 f_{m+1,n} + 810 f_{m+2,n} - 1235 f_{m+3,n} + 1130 f_{m+4,n} \\ - 621 f_{m+5,n} + 190 f_{m+6,n} - 25 f_{m+7,n}),$$

$$c_8 = \frac{1}{40,320h^6} (4 f_{m,n} - 27 f_{m+1,n} + 78 f_{m+2,n} - 125 f_{m+3,n} + 120 f_{m+4,n} \\ - 69 f_{m+5,n} + 22 f_{m+6,n} - 3 f_{m+7,n}),$$

$$c_9 = -\frac{1}{362,880h^7} (f_{m,n} - 7 f_{m+1,n} + 21 f_{m+2,n} - 35 f_{m+3,n} + 35 f_{m+4,n} \\ - 21 f_{m+5,n} + 7 f_{m+6,n} - f_{m+7,n})$$

References

1. Ahmed, B.S.; Monaque, S.J. Fourth Order Accurate Scheme with Multigrid Method for Solving Anisotropic Elliptic Partial Differential Equations. *Adv. Differ. Equ. Control Process.* **2010**, *5*, 103–110.
2. Juraev, D.A.; Gasimov, Y.S. On the regularization Cauchy problem for matrix factorizations of the Helmholtz equation in a multidimensional bounded domain. *Azerbaijan J. Math.* **2022**, *12*, 142–161.
3. Musaev, H.K. The Cauchy problem for degenerate parabolic convolution equation. *TWMS J. Pure Appl. Math.* **2021**, *12*, 278–288.
4. Pankov, P.S.; Zheentaeva, Z.K.; Shirinov, T. Asymptotic reduction of solution space dimension for dynamical systems. *TWMS J. Pure Appl. Math.* **2021**, *12*, 243–253.
5. Adiguzel, R.S.; Aksoy, U.; Karapinar, E.; Erhan, I.M. On the solutions of fractional differential equations via Geraghty type hybrid contractions. *Appl. Comput. Math.* **2021**, *20*, 313–333.
6. Ozyapici, A.; Karanfiller, T. New integral operator for solution of differential equations. *TWMS J. Pure Appl. Math.* **2020**, *11*, 131–143.
7. Quinlan, J.E. Variable Compact Multi-Point Upscaling Schemes for Anisotropic Diffusion Problems in Three-Dimensions. Ph.D. Thesis, University of Southern Mississippi, Hattiesburg, MS, USA, 2020. Available online: <https://aquila.usm.edu/dissertations/1800> (accessed on 30 June 2022).
8. Bourantas, G.C.; Burganos, V.N. An implicit meshless scheme for the solution of transient non-linear poisson-type equations. *Eng. Anal. Bound. Elem.* **2013**, *37*, 1117–1126. [\[CrossRef\]](#)
9. Aziz, I.; Islam, S. An efficient Modified Haar Wavelet Collocation Method for Numerical Solution of Two-dimensional Elliptic PDEs. *Differ. Equ. Dyn. Syst.* **2015**, *4*, 39–50. [\[CrossRef\]](#)

10. Faydaoglu, S.; Ozis, T. Periodic solutions for certain non-smooth oscillators with high nonlinearities. *Appl. Comput. Math.* **2021**, *20*, 366–380.
11. Zargari, E.A.; Jimack, P.K.; Walkley, M.A. An investigation of the film thickness calculation for elastohydrodynamic lubrication problems. *Int. J. Numer. Methods Fluids* **2007**, 1–6. Available online: <https://citeseerx.ist.psu.edu/viewdoc/download?doi=10.1.1.67.2470&rep=rep1&type=pdf> (accessed on 30 June 2022).
12. Datta, S. *Quantum Transport: Atom to Transistor*; Cambridge University Press: London, UK, 2015.
13. Iskenderov, N.S.; Allahverdiyeva, S.I. An inverse boundary value problem for the boussinesq-love equation with nonlocal integral condition. *TWMS J. Pure Appl. Math.* **2020**, *11*, 226–237.
14. Qalandarov, A.A.; Khaldjigitov, A.A. Mathematical and numerical modeling of the coupled dynamic thermoelastic problems for isotropic bodies. *TWMS J. Pure Appl. Math.* **2020**, *11*, 119–126.
15. Ashyralyev, A.; Agirseven, D.; Agarwal, R.P. Stability estimates for delay parabolic differential and difference equations. *Appl. Comput. Math.* **2020**, *19*, 175–204.
16. Duan, J.; Rach, R. A new modification of the Adomian decomposition method for solving boundary value problems for higher order nonlinear differential equations. *Appl. Math. Comput.* **2011**, *218*, 4090–4118. [\[CrossRef\]](#)
17. Tatari, M.; Dehghan, M. The use of the Adomian decomposition method for solving multipoint boundary value problems. *Phys. Scr.* **2006**, *73*, 672–676. [\[CrossRef\]](#)
18. Saparova1, B.; Mamytova1, R.; Kurbanbaeva, N.; Ahmedov, A.A. A Haar Wavelet Series Solution of Heat Equation with Involution. *J. Adv. Res. Fluid Mech. Therm. Sci.* **2021**, *86*, 50–55. [\[CrossRef\]](#)
19. Ramos, H.; Abdulganiy, R.; Olowe, R.; Jator, S. A family of functionally-fitted third derivative block falkner methods for solving second-order initial-value problems with oscillating solutions. *Mathematics* **2021**, *9*, 713. [\[CrossRef\]](#)
20. Shokri, A.; Saadat, H.; Khodadadi, A. A new high order closed Newton-Cotes trigonometrically-fitted formulae for the numerical solution of the Schrodinger equation. *Iranian J. Math. Sci. Inform.* **2018**, *13*, 111–129.
21. Yousif, M.A.; Mahmood, B.A. Approximate solutions for solving the Klein-Gordon and sine-Gordon equations. *J. Assoc. Arab. Univ. Basic Appl. Sci.* **2017**, *22*, 83–90. [\[CrossRef\]](#)
22. Martinsson, P. A direct solver for variable coefficient elliptic PDEs discretized via a composite spectral collocation method. *J. Comput. Phys.* **2013**, *242*, 460–479. [\[CrossRef\]](#)
23. Abolarin, O.E.; Kuboye, J.O.; Adeyefa, E.O.; Ogunware, B.G. New efficient numerical model for solving second, third and fourth order ordinary differential equations directly. *Gazi J. Sci.* **2020**, *33*, 821–833. [\[CrossRef\]](#)
24. Ukpebor, L.A.; Omole, E.O. Three-step Optimized Block Backward Differentiation Formulae (TOBBDF) for Solving Stiff Ordinary Differential Equations. *Afr. J. Math. Comput. Sci. Res.* **2020**, *13*, 51–57. [\[CrossRef\]](#)
25. Modebei, M.I.; Adeniyi, R.B. A Six-step block unification integrator for numerical solution of fourth order boundary value problems. *Gen. Lett. Math.* **2018**, *5*, 71–83. [\[CrossRef\]](#)
26. Aigbiremhon, A.A.; Familua, A.B.; Omole, E.O. A three-step interpolation technique with perturbation term for direct solution of third-order ordinary differential equations. *FUDMA J. Sci.* **2021**, *5*, 365–376. [\[CrossRef\]](#)
27. Sunday, J.; Shokri, A.; Marian, D. Variable Step Hybrid Block Method for the Approximation of Kepler Problem. *Fractal Fract.* **2022**, *6*, 343. [\[CrossRef\]](#)
28. Sun, H.; Zhang, J. A high order finite difference discretization strategy based on extrapolation for convection diffusion equations. *Numer. Methods Partial. Differ. Equ.* **2004**, *20*, 18–32. [\[CrossRef\]](#)
29. Marian, D.; Semi-Hyers-Ulam-Rassias, D. Stability of the Convection Partial Differential Equation via Laplace Transform. *Mathematics* **2021**, *9*, 2980. [\[CrossRef\]](#)
30. Raslan, K.R.; Ali, K.K.; Al-Bayatti, H.M.Y. Construct extended cubic B-splines in n-dimensional for solving n-Dimensional partial differential equations. *Appl. Math. Inf. Sci.* **2021**, *15*, 599–611.
31. Kamran, M.; Abbas, M.; Majeed, A.; Emadifar, H.; Nazir, T. Numerical Simulation of Time Fractional BBM-Burger Equation Using Cubic B-Spline Functions. *Hindawi J. Funct. Spaces* **2022**, *2022*, 2119416. [\[CrossRef\]](#)
32. Rashidinia, J.; Mohammadi, R. Sextic spline solution of variable coefficient fourth-order parabolic equations. *Int. J. Comput. Math.* **2010**, *87*, 3443–3454. [\[CrossRef\]](#)
33. Lambert, J.D. *Computational Methods in Ordinary Differential Equations*; John Wiley & Sons Inc.: Hoboken, NJ, USA, 1973.
34. Henrici, P. *Discrete Variable Method in Ordinary Differential Equations*; John Wiley and Sons: New York, NY, USA, 1962.
35. Salzer, H.E.; Zucker, R.; Capuano, R. Table of the zeros and weight factors of the first twenty Hermite polynomials. *J. Res. Nat. Bur. Stand.* **1952**, *48*, 111–116. [\[CrossRef\]](#)
36. Fatunla, S.O. *Numerical Methods for Initial Value Problems in Ordinary Differential Equations*; Academic Press Inc.: Cambridge, MA, USA; Harcourt Brace Jovanovich Publishers: New York, NY, USA, 1988.
37. Omole, E.O.; Jeremiah, O.A.; Adoghe, L.O. A Class of Continuous Implicit Seventh-eight method for solving $y' = f(x, y)$ using power series as basic function. *Int. J. Chem. Math. Phys. (IJCMP)* **2020**, *4*, 39–50. [\[CrossRef\]](#)
38. Ramos, H.; Vigo-Aguiar, J. An almost L-stable BDF-type method for the numerical solution of stiff ODEs arising from the method of lines. *Int. J. Numer. Methods Partial. Differ. Equ.* **2006**, *23*, 1110–1121. [\[CrossRef\]](#)

-
39. Wang, Y.; Zhang, J. Sixth order compact scheme combined with multigrid method and extrapolation technique for 2D poisson equation. *J. Comput. Phys.* **2009**, *228*, 137–146. [[CrossRef](#)]
 40. Ashry, H.; Abd-Elhameed, W.M.; Moatimid, G.M.; Youssri, Y.H. Spectral Treatment of One and Two Dimensional Second-Order BVPs via Certain Modified Shifted Chebyshev Polynomials. *Int. J. Appl. Comput. Math.* **2021**, *7*, 248. [[CrossRef](#)]